

## Glassy dynamics in granular compaction

Anita Mehta<sup>†</sup> and G C Barker<sup>‡</sup>

<sup>†</sup> S N Bose National Centre for Basic Sciences, Block JD, Sector III, Salt Lake, Calcutta 700091, India

<sup>‡</sup> Institute of Food Research, Norwich Research Park, Colney Lane, Norwich NR4 7UA, UK

E-mail: anita@boson.bose.res.in and barker@bbsrc.ac.uk

Received 2 March 2000

**Abstract.** Two models are presented for studying the influence of slow dynamics on granular compaction. It is found in both cases that high values of packing fraction are achieved only by the slow relaxation of cooperative structures. Ongoing work investigating the full implications of these issues is discussed.

### 1. Introduction

The importance of glassy dynamics in granular media was recognized well before recent experiments [1–3] in granular compaction [4] made some of the underlying ideas concrete [5,6]. In particular, the idea that *two* dynamical mechanisms are needed to explain some of the observed experimental phenomena [7] has previously been put forward [8]; a cooperative mechanism embodies the slow dynamics of relaxing granular clusters, while a single-particle mechanism represents mobile grains moving between clusters.

In this paper, we discuss the results from two models that incorporate glassy dynamics into the phenomenon of granular compaction. Our first approach is based on a hybrid Monte Carlo dynamics (which contains both single-particle and cooperative components), and the second uses a cellular automaton model, that includes, in addition to the canonical threshold-driven grain flow, a representation of cooperative reorganization via dynamical disorder. In both cases, we find that a driven sandpile undergoes compaction largely as a result of the slow dynamics of cooperative motion.

While it has been shown in earlier work that granular compaction beyond values of packing fraction of 0.56 occurs almost entirely because of the cooperative relaxation of grain clusters [9], the present results from Monte Carlo simulations shed some light on the details of this compaction in relation to experiments [1,2]. Equally, on realizing that the analogue of bulk compaction corresponds to smoothing of the sandpile surface, we demonstrate that this is indeed what occurs in our driven and dynamically disordered cellular automaton model.

### 2. Bulk compaction: a hybrid Monte Carlo model

Recent experiments [1–3] have demonstrated the importance of glassy dynamics in granular compaction. In reference [1], the authors observed a monotonic increase of packing fraction with excitation intensity. In references [2,3], a more complex (and now well-established) behaviour was observed: an initial ramping up of the intensity led, as before, to an increase

of volume fraction. However, at a certain point (the ‘irreversibility point’) any subsequent increase of volume fraction could only be generated by *decreasing* the intensity of vibration. The first of these two regimes, called the irreversible branch, was interpreted as the increase in packing fraction resulting from the shaking out of voids from an initial, loosely packed state. The second regime, called the reversible branch, is in accord with the earlier predictions of Monte Carlo simulations [9, 10]; one of the features of the reversible branch, as its name implies, is that evolution in the directions of either increasing or decreasing excitation intensity yields reproducible results for the packing fraction. Monte Carlo simulations are predicated on reversible transitions between configurations, so their predictions lie entirely on the reversible branch of the experimental curves.

In this paper, we take these investigations further in a bid to understand the theoretical implications of the experimental phase diagram. We find a transition point in the behaviour of a shaken sphere packing; for a range of shaking intensities, there is a transition to an ordered close-packed state (with packing fractions  $\phi \geq 0.61$ ) after sufficiently long shaking times. For intensities below this range the powder remains stuck in some configurations and therefore cannot crystallize: for intensities above this range, the behaviour is analogous to ‘quenching’ and crystallization is therefore inhibited. We argue that the lower bound for this range of shaking intensities corresponds to the ‘irreversibility point’ observed in experiments [2].

Our simulations use uniform hard spheres, subjected to non-sequential reorganizations which represent the effect of shaking. A variable shaking amplitude  $A$  is parametrized in units of the particle diameter; thus for example,  $A = 1.0$  means that shaken particles are able to move longitudinally and laterally by, on average, one particle diameter (subject to volume exclusions) during a shake cycle. The details of the shaking algorithm have been discussed elsewhere [9, 11]. Briefly, one cycle of vibration of the granular assembly (corresponding to one time step of our simulation) is modelled by:

- (a) a vertical dilation of the granular bed, in proportion to the shaking amplitude  $A$ ;
- (b) a stochastic rearrangement of the individual particles in transverse directions, with available free volume proportional once again to the shaking amplitude;
- (c) and finally a *cooperative* recompression of the assembly as each grain lands on the substrate alone or with neighbours; in the latter case, arches would form.

In conventional Monte Carlo simulations, the cooperative step is absent, and particle reorganization is sequential; this corresponds to a regime of ‘fast’ dynamics, driven by the inertia of the grains. In contrast, our simulations interpolate naturally from this regime to one with slow dynamics, characteristic of that found in glassy motion, because of the inclusion of cooperative rearrangements in the last step. In regions where the shaking amplitude  $A$  is large, one can discuss the dynamics in terms of the motion of the individual particles, since any arches that form at one time step are rapidly destroyed at another, i.e. there is little indication of long-lived cooperative motion. In contrast, for low shaking amplitudes, the cooperative step which we have added to our Monte Carlo procedure is crucially important for modelling the correlated motion of grains that is important in slow dynamics. In earlier work we have studied this slow dynamics using displacement correlation functions, and thus defined the concept of a dynamical cluster [10]. Similar displacement correlations have subsequently been studied in the context of glasses [12]. This crossover between the fast and slow dynamics can be viewed also in terms of the interpolation between two effective temperatures in a granular medium, the first corresponding to the conventional granular temperature defined in terms of the inertia of the grains [13], and a second corresponding to a density-related temperature first defined by Edwards [14], and known as the compactivity. The details of such interpolation are discussed analytically elsewhere [15]; a recent approach which looks at the issue of two temperatures at

a more microscopic level is due to Kurchan [16].

We now present our simulation results. Starting from a random loose packing with packing fraction  $\phi \sim 0.54$ , a fixed shaking intensity leads to packings with steady-state values for the packing fraction. The steady state is approached after short or long transients, depending on the value of shaking intensity. However, within a range of excitation intensities, further shaking for extended periods may produce a jump to an ordered close-packed state; we term this shaking-induced crystallization. (Clearly, the word ‘crystallization’ is used here and in what follows in a very loose sense since we mean simply that the nature of the observed order is qualitatively different from that corresponding to random close packing; see figure 2.) Outside this range, we have not observed crystallization, at least for our simulation times, though we speculate that for extremely long times, and for shaking intensities *below* our range, a jump to the crystalline state could be a possibility (see below).

Our simulations are carried out in an  $8 \times 8 \times 8$  periodic box filled with monosize unit spheres; there are approximately 700 spheres in total. Figure 1 shows the variation of the

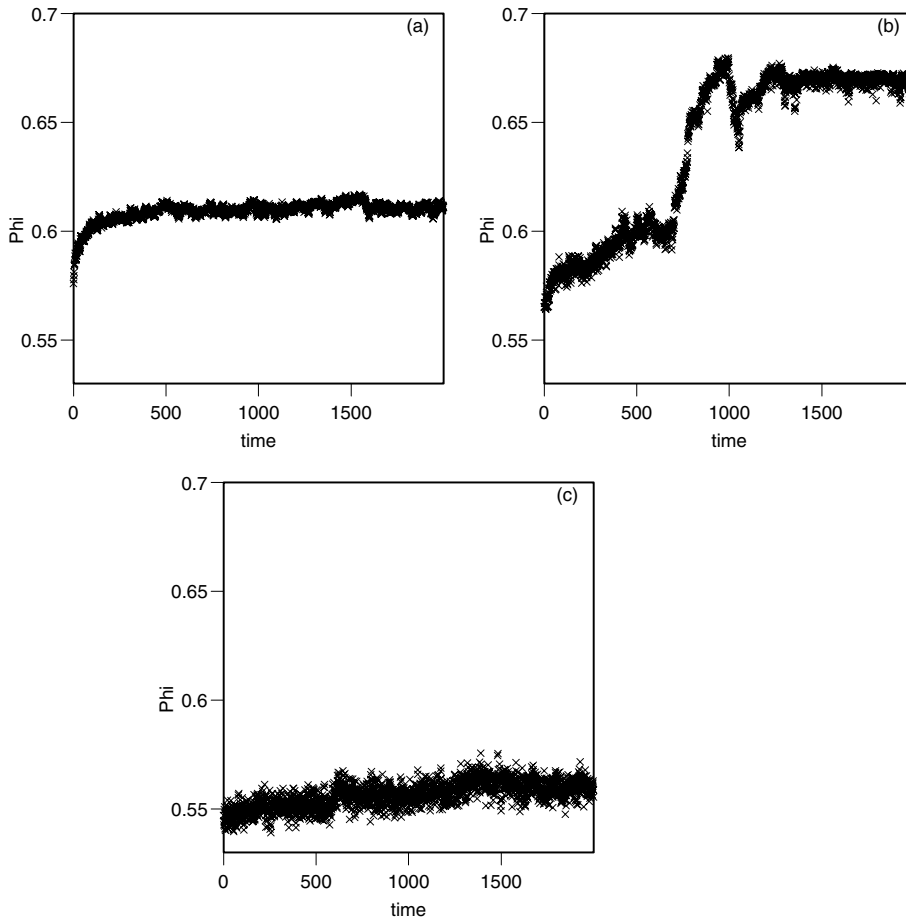


**Figure 1.** Plots of packing fraction  $\phi$  versus time  $t$  for (a)  $A = 0.05$ , (b)  $A = 0.5$ , (c)  $A = 1.2$ . Note the approach to crystallization in (b).

packing fraction with time  $t$  (in shaking cycles), as the spheres are shaken, at amplitudes  $A = 0.05, 0.5$  and  $1.2$  respectively. For  $A = 0.5$  (figure 1(b)), we notice a sharp rise in packing fraction to about  $\phi = 0.68$  at  $t \sim 900$ . This does not happen in the other two cases, at least for our times of observation. (At the lowest shaking intensity we have followed the time series for  $2 \times 10^5$  cycles). For large shaking amplitudes (figure 1(c)), the dynamics is akin to that of fluidization, while for very small  $A$ , the granular bed appears to be stuck in ‘supercooled’ configurations. These results indicate that there is a range of amplitudes that will allow for the granular assembly to crystallize; clearly this depends on the observation time, since, at very low shaking intensity, we cannot rule out a jump to the near-crystalline state from one of the supercooled states over infinitely long times.

In figure 2, we show clusters of approximately 300 spheres generated at  $t = 2000$ , corresponding respectively to  $A = 0.05$  and  $A = 0.5$ . In the latter case, the snapshot is taken after the ordering transition. The structures are fundamentally different, leading to our conjecture that the latter corresponds to an ordered state. The increase in order seen in figure 2(b) lends weight to the existence of the ‘maximally jammed’ state recently postulated by Torquato *et al* [27], where the accessibility of states substantially beyond random close packing can be reached, at the expense of disorder.

These results lend weight to a conjecture that, as in glasses, a barrier height distribution [15] exists between configurations; at very low intensities of vibration, the driving force cannot typically force the system to cross barriers, leading to ‘stuck’ configurations in the powder, which look supercooled. These barriers are entropic, and the barrier height represents the energy threshold needed to move the system from one configuration to another. The relaxations, both for fast and slow dynamics, are expected to be activated processes over the (random) distribution of barrier heights; in each case, the appropriate effective temperature controls the kinetics [15].

As the intensity increases, the configurations can evolve more easily (the powder becomes more ergodic), so in principle, for infinite times, the system can achieve a crystalline limit. In order to understand why little compaction occurs (and why certainly the transition to the crystalline state would be most unlikely) above the allowed range, we must consider the mechanism of compaction discussed previously [10]. As the intensity of vibration decreases, fewer and fewer grains are able to break away from their clusters, so structures such as arches are long-standing even during driving. The relaxation of these arches in a cooperative sense (measured by displacement correlation functions [10]) leads to the decrease of the void space which is trapped in the arches (‘bridge collapse’) and, overall, the powder compacts. In contrast, arches make and break during strong driving (the autocorrelation function for grains decays to zero rather rapidly [10]), so there are strong fluctuations in the total volume of void space and no overall compaction results. (Another way of seeing this is that the effective temperature for such fast dynamics affects the inertia of individual grains, rather than helping the system overcome configurational barriers en route to compaction [26].) This fluctuating behaviour in the global packing fraction of the powder can be seen very clearly from figure 1(c), and was also noted in reference [3].

Further work is in progress to refine and extend these results, but we discuss below the possible relationship between the simulations and the experiment in references [2, 3]. There are important differences between our simulations and the compaction experiments. The irreversible branch of the Chicago experiments consists of transitions between states that can only be reached in one direction—this directionality corresponds to the ramping up of the reduced acceleration. The trajectories of our simulation, on the other hand, connect what we believe to be ‘equilibrium states’ (at least within our observation times), and transitions are in general reversible. This observation [2] indicates that our simulation data correspond

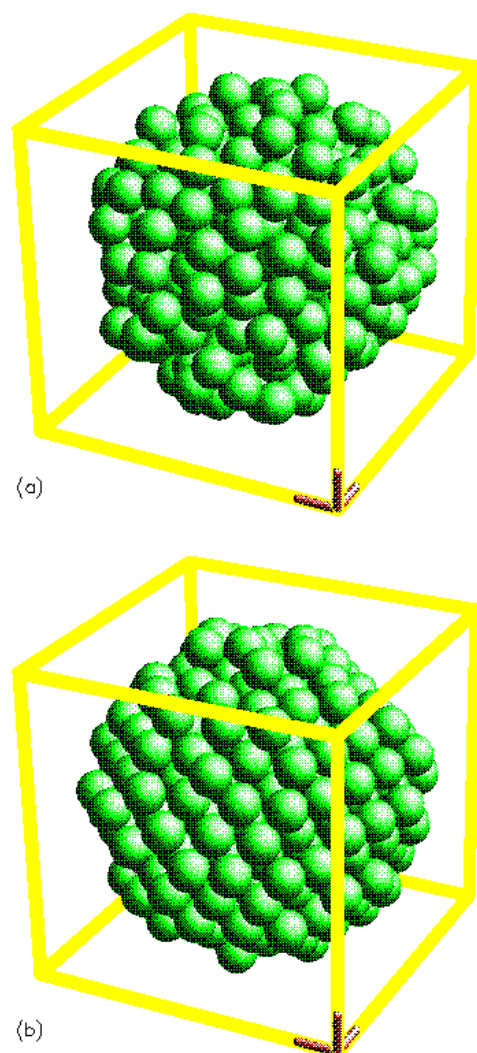


**Figure 2.** An example of typical clusters obtained after 2000 time steps for (a)  $A = 0.05$ , (b)  $A = 0.5$ . Note the crystalline-like ordering in the second case.

(This figure can be viewed in colour in the electronic version of the article; see [www.iop.org](http://www.iop.org))

to the reversible branch of the experimental graphs. Another important difference concerns the fact that our data represent the time evolution of the packing fraction of the powder at a fixed shaking intensity, while those from the Chicago experiments concern the evolution of the packing fraction as a function of the shaking intensity, and of the *time* spent at each intensity. It was noted [3] that, except at very low-intensity driving, with the consequent preponderance of ‘supercooled’ states in the powder, it may be possible to reach the reversible branch by having an extended time of excitation, at a fixed intensity.

Our results include this interesting possibility. While clearly the ‘crystallization’ observed

in figure 1(b) might be regarded as an irreversible transition (it is easier for a close-packed array to be shaken down to lower density than for a loose-packed powder to make a sudden jump—overcoming a configurational barrier—to a crystalline density), it is included in a trajectory that has reversible steps. On the other hand, for extremely low intensities, it is likely that the supercooled configurations of the powder would be persistent on the timescale of experiments. We speculate therefore that the lower bound for the range of intensities where such crystallization is possible corresponds to the irreversibility point observed in experiments [2,3].

In ongoing work [18], we have been able to reproduce the experimentally observed irreversible/reversible transition [2, 3]; we are now examining the influences of increasing observation times at fixed, low-intensity shaking, on the point at which the transition to crystallinity is observed. In addition we are making an accurate determination of the range of intensities, for different system sizes and times of observation, for which this crystallization is possible and we are mimicking the experiment by looking at varying shaking intensities at fixed ramp rates. We hope in this way to determine the value of the irreversibility point, as well as the behaviour of the system around it.

### 3. Surface compaction: a disordered cellular automaton model

We now examine the issue of ‘surface compaction’, or smoothing of a driven sandpile surface. As deposition occurs on a sandpile surface, clusters of grains grow unevenly at different positions and roughness builds up until further deposition renders some of the clusters unstable. These then start ‘toppling’, so grains from an already unstable cluster flow down the sandpile, knocking off grains from other similar clusters which they encounter. The net effect of this is to ‘wipe off’ protrusions (where there is a surfeit of grains at a cluster) and to ‘fill in’ dips, where the oncoming avalanche can disburse some of its grains. In short, the surface is smoothed by the passage of the avalanche, so there is a rough precursor surface, and a smoothed post-avalanche surface.

We have used a cellular automaton (CA) model [17] of an evolving sandpile to examine this issue; this model appears [18] to be the discrete version of an earlier continuum model [19]. This CA model is a ‘disordered’ version of the basic Kadanoff cellular automaton [20]; a further degree of freedom, that involves granular reorganization within columns, is added to the basic model which includes only granular flow between columns. As in the previous section, this extra ingredient of intra-column reorganization is a way to introduce slow cooperative dynamics into the system. As we will see, these orientational relaxations cause surface smoothing of our CA sandpile, mirroring the way in which the cooperative step in the Monte Carlo procedure caused the observed bulk compaction (see above).

Our disordered model sandpile<sup>†</sup> is built from rectangular lattice grains, that have aspect ratio  $a \leq 1$ , arranged in columns  $i$  with  $1 \leq i \leq L$ , where  $L$  is the system size. Each grain is labelled by its column index  $i$  and by an orientational index 0 or 1, corresponding respectively to whether the grain rests on its larger or smaller edge. The two grain orientations represent regions of either loose-packed (type 1) or close-packed (type 0) material.

The dynamics of our model has been described at length elsewhere [17]; briefly,

- Grains are deposited on the sandpile with fixed probabilities for orientation in the 0 or 1 states.
- The incoming grains, as well as all the grains in the same column, can then ‘flip’ to the other orientation stochastically (with probabilities which decrease with depth from the surface).

This ‘flip’, or change of orientation, is our simple representation of *collective dynamics*

<sup>†</sup> Disordered sandpiles described here have parameters [17]  $z_0 = 2$ ,  $z_1 = 20$  and  $a = 0.7$ , unless otherwise stated.

in granular clusters since typically clusters reorganize owing to the slight orientational movements of the grains within them [11]. The transition probabilities in this case involve scale heights which are weighted so as to favour the destruction of voids, as in a slowly consolidating granular material [21].

- The height of column  $i$  at time  $t$ ,  $h(i, t)$ , can be expressed in terms of the instantaneous numbers of 0 and 1 grains,  $n_0(i, t)$  and  $n_1(i, t)$  respectively:

$$h(i, t) = n_1(i, t) + an_0(i, t) \quad (1)$$

- Finally, grains fall to the next column down the sandpile (maintaining their orientation as they do so) if the height difference exceeds a specified threshold in the normal way [20] (the pile is local, limited and has a fall number of two). At this point, avalanching may occur.

We begin with the principle of dynamical scaling for sandpile cellular automata [18] in terms of the surface width  $W$  of the sandpile automaton:

$$W(t) \sim t^\beta \quad t \ll t_{crossover} \equiv L^z \quad (2)$$

$$W(L) \sim L^\alpha \quad L \rightarrow \infty \quad (3)$$

As in the case of interfacial widths, these equations signify the following sequence of roughening regimes:

- To start with, roughening occurs at the CA sandpile surface in a time-dependent way; after an initial transient, the width scales asymptotically with time  $t$  as  $t^\beta$ , where  $\beta$  is the *temporal roughening* exponent. This regime is appropriate for all times less than the crossover time  $t_{crossover} \equiv L^z$ , where  $z = \alpha/\beta$  is the dynamical exponent and  $L$  the system size.
- After the surface has *saturated*, i.e. when its width no longer grows with time, the *spatial roughening* characteristics of the mature interface can be measured in terms of  $\alpha$ , an exponent characterizing the dependence of the width on  $L$ .

We define the surface width  $W(t)$  for a sandpile automaton in terms of the mean squared deviations from a suitably defined mean surface; in analogy with the conventional counterpart for interface growth [22], we define the instantaneous mean surface of a sandpile automaton as the surface about which the sum of column *height* fluctuations vanishes. Clearly, in an evolving surface, this must be a function of time; hence all quantities in the following analysis will be presumed to be instantaneous.

The mean slope  $\langle s(t) \rangle$  defines expected column heights,  $h_{av}(i, t)$ , according to

$$h_{av}(i, t) = i \langle s(t) \rangle \quad (4)$$

where we have assumed that column 1 is at the bottom of the pile. Column height deviations are defined by

$$dh(i, t) = h(i, t) - h_{av}(i, t) = h(i, t) - i \langle s(t) \rangle. \quad (5)$$

The mean slope must therefore satisfy

$$\sum_i [h(i, t) - i \langle s(t) \rangle] = 0 \quad (6)$$

since the instantaneous deviations about it vanish; thus

$$\langle s(t) \rangle = 2 \sum_i [h(i, t)] / L(L + 1). \quad (7)$$

The instantaneous width of the surface of a sandpile automaton,  $W(t)$ , can be defined as

$$W(t) = \sqrt{\sum_i [dh(i, t)^2]/L} \quad (8)$$

which can in turn be averaged over several realizations to give  $\langle W \rangle$ , the average surface width in the steady state.

Figure 3(a) shows a time series for the mass of a large ( $L = 256$ ) evolving disordered sandpile automaton. The series has a typical quasiperiodicity [23]. The vertical line denotes the position of a particular ‘large’ event, while figure 3(b) shows the avalanche size distribution for the sandpile. Note the peak, corresponding to the preferred large avalanches, which was analysed extensively in earlier work [17]. Our data show that the avalanche highlighted in figure 3(a) drained off approximately five per cent of the mass of the sandpile, placing it close to the ‘second peak’ of figure 3(b). Figure 3(c) shows the outline of the full avalanche before and after this event with its initiation site marked by an arrow; we note that, as is often the case in one dimension, the avalanche is ‘uphill’. The inset shows the relative motion of the surface during this event; we note that the signatures of smoothing by avalanches are already evident as the precursor state in the inset is much rougher than the final state. Finally we show in figure 3(d) the grain-by-grain picture of the aftermath pile superposed on the precursor pile, which is shown shaded. An examination of the aftermath pile and the precursor pile shows that the propagation of the avalanche across the upper half of the pile has left only a very few disordered sites in its wake (i.e. the majority of the remaining sites are type 0), whereas the lower half (which was undisturbed by the avalanche) still contains many disordered (i.e. type 1) sites in the boundary layer. This leads us to suggest that the larger avalanches rid the boundary layer of its disorder-induced roughness, a fact that is borne out by our more quantitative investigations. In fact, our studies have revealed that the very largest avalanches, which are system spanning, remove virtually all disordered sites from the surface layer; one is then left with a normal ‘ordered’ sandpile, where the avalanches have their usual scaling form for as long as it takes for a layer of disorder to build up. When the disordered layer reaches a critical size, another large event is unleashed; this is the underlying reason for the quasiperiodic form of the time series shown in figure 3(a).

The *bulk* packing fraction  $\phi$  of the disordered sandpile increases after a large event, i.e. effective consolidation occurs during avalanching. Internal consolidation and surface smoothing are, therefore, closely related. Also, a comparison of the surface width for pre- and post-large-event sandpiles shows that the surface width goes down considerably during an event, once again suggesting that a rough precursor pile is smoothed by the propagation of a large avalanche.

We turn finally to the measurement of the critical exponents defined above.

Our results are [18]:

- For disordered sandpiles ( $L = 2048$ ) we find  $\beta = 0.42 \pm 0.05$ ; for ordered sandpiles ( $L = 2048$ )  $\beta = 0.17 \pm 0.05$ .
- For disordered sandpiles above a crossover size of  $L_c = 90$  we find  $\alpha = 0.723 \pm 0.04$ , while for ordered piles we find  $\alpha = 0.356 \pm 0.05$ .
- On the basis of the above values we find that the dynamical exponent,  $z$ , has values of  $1.72 \pm 0.29$  and  $2.09 \pm 0.84$  for the disordered and ordered sandpiles.

Since the effect of large avalanches is to transform a disordered pile into a largely ordered one (figure 3), we notice that the above exponents confirm the smoothing of the surface. It is important to realize that it is the mechanism of column reorganization, our representation of the slow dynamics of the system, that causes the initial accumulation of grains resulting in

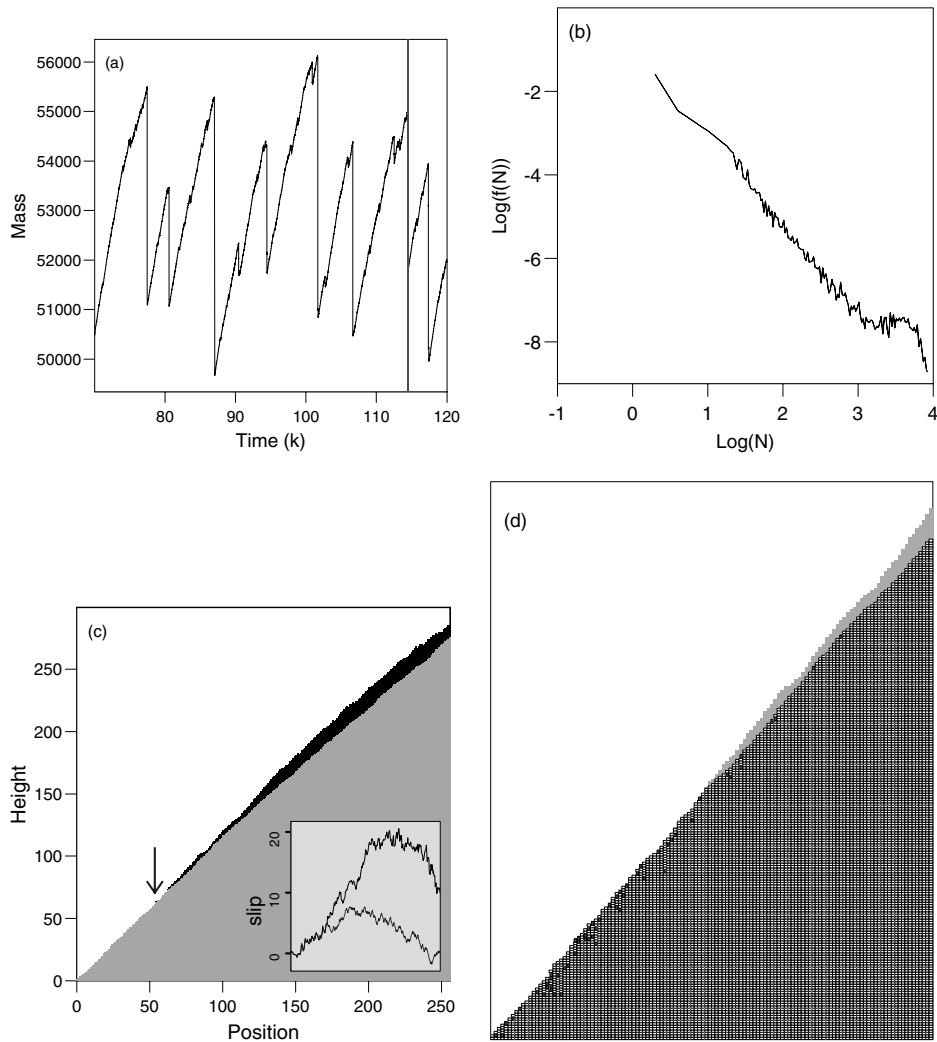


**Figure 3.** (a) A time series of the mass for a model sandpile ( $L = 256$ ) that has been built to include a surface layer containing structural disorder. The vertical line indicates the position in this series of the large avalanche illustrated in (c), (d). (b) A log–log plot of the event size distribution for a model sandpile ( $L = 256$ ) that includes a surface layer containing structural disorder. (c) An illustration of a large wedge-shaped avalanche in a model sandpile ( $L = 256$ ) that has been built to include a surface layer containing structural disorder. A lighter aftermath pile has been superposed onto the dark precursor pile and an arrow shows the point at which the event was initiated. The inset shows the relative positions of the two surfaces and their relationship to a pile that has a smooth slope. (d) A detailed picture of the internal structure of a model sandpile in the aftermath of a large avalanche event. The individual grains of the aftermath pile (for columns 1–128 of a sandpile with  $L = 256$ ) are superposed on the grey outline of the precursor pile. The black squares represent type 1 (disordered grains).

the roughness of the precursor surface, and thus the eventual smoothing of the surface. We emphasize that the addition of such slow dynamics, independent of model details, is expected to

have similar consequences. For example, the crucial role of the cooperative mechanism has also been confirmed in recent analytical investigations of the asymptotic smoothing of continuum sandpile surfaces [24]; it has also been seen to influence the geometrical features of two-dimensional model avalanches [18] (cf. recent experiments on sloping beds of spheres [25]).

### Acknowledgment

GCB acknowledges support from the BBSRC, UK (218/OF6522).

### References

- [1] Knight J B, Fandrich C G, Lau C N, Jaeger H M and Nagel S R 1995 *Phys. Rev. E* **51** 3957
- [2] Nowak E R, Knight J B, Ben-Naim E, Jaeger H M and Nagel S R 1998 *Phys. Rev. E* **57** 1971
- [3] Nowak E R, Knight J B, Povinelli M, Jaeger H M and Nagel S R 1997 *Powder Technol.* **94** 79
- [4] Jaeger H M, Nagel S R and Behringer R P 1996 *Rev. Mod. Phys.* **68** 1259
- [5] Boutreux T, Raphaël E and de Gennes P-G 1998 *Phys. Rev. E* **58** 4692
- Aradian A, Raphaël E and de Gennes P-G 1999 *Phys. Rev. E* **60** 2009
- [6] Edwards S F and Grinev D V 1999 *Phys. Rev. E* **58** 4758
- [7] Jaeger H M, Liu C and Nagel S R 1989 *Phys. Rev. Lett.* **62** 40
- [8] Mehta A 1992 *Physica A* **186** 121
- [9] Mehta A and Barker G C 1991 *Phys. Rev. Lett.* **67** 394
- [10] Barker G C and Mehta A 1992 *Phys. Rev. A* **45** 3435
- Barker G C and Mehta A 1993 *Phys. Rev. E* **47** 184
- [11] Mehta A (ed) 1994 *Granular Matter: an Interdisciplinary Approach* (New York: Springer)
- [12] Kob W, Donati C, Plimpton S J, Poole P H and Glotzer S C 1997 *Phys. Rev. Lett.* **79** 2827
- [13] See e.g.
  - Savage S B 1994 *Adv. Appl. Mech.* **24** 289 and references therein
- [14] Edwards S F 1994 *Granular Matter: an Interdisciplinary Approach* ed A Mehta (New York: Springer)
- [15] Mehta A, Needs R J and Dattagupta S 1992 *J. Stat. Phys.* **68** 1131
- [16] See the article by Jorge Kurchan elsewhere in this Special Issue:
  - Kurchan J 2000 *J. Phys.: Condens. Matter* **12** 6611
- [17] Mehta A and Barker G C 1994 *Europhys. Lett.* **27** 501
- Mehta A, Barker G C, Luck J M and Needs R J 1996 *Physica A* **224** 48
- [18] Barker G C and Mehta A 1999 unpublished
- [19] Mehta A, Luck J M and Needs R J 1996 *Phys. Rev. E* **53** 92
- [20] Kadanoff L P, Nagel S R, Wu L and Zhou S-M 1989 *Phys. Rev. A* **39** 6254
- Bak P, Tang C and Wiesenfeld K 1988 *Phys. Rev. A* **38** 368
- [21] Buscall R 1990 *Colloids Surf.* **43** 33
- Snyder R E and Ball R C 1994 *Phys. Rev. E* **49** 104
- Edwards S F and Grinev D V 1998 *Phys. Rev. E* **58** 4758
- [22] Krug J 1997 *Adv. Phys.* **46** 1
- [23] Held G A, Solina D H, Keane D T, Haag W J, Horn P M and Grinstein G 1990 *Phys. Rev. Lett.* **65** 1120
- [24] Biswas P, Majumdar A, Mehta A and Bhattacharjee J K 1998 *Phys. Rev. E* **58** 1266
- [25] Daerr A and Douady S 1999 *Nature* **399** 241
- [26] Head D A and Rogers G J 1998 *J. Phys. A: Math. Gen.* **31** 107
- [27] Torquato S, Truskett T M and Debenedetti P G 2000 *Phys. Rev. Lett.* **84** 2064